

Dosimetric Comparison of Integral Radiation Dose: Anisotropic Analytical Algorithm and Acuros XB in Breast Radiotherapy

Aydin Cakir^{1*}, Zuleyha Akgun²

¹Istanbul Bilgi University, Istanbul, Turkey

²Istanbul Memorial Hospital, Istanbul, Turkey

Email: *aydin.cakir@bilgi.edu.tr

How to cite this paper: Cakir, A. and Akgun, Z. (2019) Dosimetric Comparison of Integral Radiation Dose: Anisotropic Analytical Algorithm and Acuros XB in Breast Radiotherapy. *International Journal of Medical Physics, Clinical Engineering and Radiation Oncology*, 8, 57-67. <https://doi.org/10.4236/ijmpcero.2019.82006>

Received: February 4, 2019

Accepted: March 23, 2019

Published: March 26, 2019

Copyright © 2019 by author(s) and Scientific Research Publishing Inc. This work is licensed under the Creative Commons Attribution International License (CC BY 4.0).

<http://creativecommons.org/licenses/by/4.0/>



Open Access

Abstract

The impact of the difference between Anisotropic Analytical Algorithm (AAA) and Acuros XB (AXB) in breast radiotherapy is not clearly due to different uses and further research is required to explain this effect. The aim of this study is to investigate the contribution of calculation differences between AAA and AXB to the integral radiation dose (ID) on critical organs. Seven field intensity modulated radiotherapy (IMRT) plans were generated using with AAA and AXB algorithms for twenty patients with early stage left breast cancer after breast conserving surgery. Volumetric and dosimetric differences, as well as, the D_{mean} , V_5 , V_{20} doses of the left and right-sided lung, the D_{mean} , V_{10} , V_{20} , V_{30} doses of heart and the D_{mean} , V_5 , V_{10} doses of the contralateral breast were investigated. The mean dose (D_{mean}), V_5 , V_{20} doses of the left-sided lung, the D_{mean} , V_5 , V_{10} doses of right-sided lung, the D_{mean} , V_{10} , V_{20} , V_{30} doses of heart and the D_{mean} , V_5 , V_{10} doses of the contralateral breast were found to be significantly higher with AAA. In this research integral dose was also higher in the AAA recalculated plan and the AXB plan with the average dose as follows left lung 2%, heart 2%, contralateral breast 8%, contralateral lung 4% respectively. Our study revealed that the calculation differences between Acuros XB (AXB) and Anisotropic Analytical Algorithm (AAA) in breast radiotherapy caused serious differences on the stored integral doses on critical organs. In addition, AXB plans showed significantly dosimetric improvements in multiple dosimetric parameters.

Keywords

Anisotropic Analytical Algorithm, Acuros XB, Breast Radiotherapy, Integral Radiation Dose

1. Introduction

Radiotherapy contributes to reducing the risk of local recurrence after surgery in the treatment of early stage breast cancer. Because of the proximity of surrounding tissues, the chest region has a very heterogeneous structure. Because of this region that contains heterogeneous tissues such as the treatment area, skin, lung, heart, and also anatomical difficulties; breast radiotherapy is difficult to apply. Depending on the technique used during breast radiotherapy, healthy tissues can take wide place in the treatment area; thus healthy tissues in and around the treatment area can be exposed to high integral doses.

The integral dose (ID) is the volume integral of the dose stored in a medium and it is equal to multiplication of the mean dose and volume in the medium in which the radiation is applied at any doses. The integral dose is also the area under the curve of a differential dose absolute-volume histogram. It is often stated that a large number of beam and monitor units (MU) used in IMRT cause an increase in ID and that the photon rays with high energy principally reduce the ID. D'Souza *et al.* reported that the change in ID with four or more beams is <1% as a function of the number of beams. As expected; high energy rays reduce the ID; they showed that the ID value was 1.5% - 1.7% for nasopharynx, 0.9% - 1.0% and 0.3% for the pancreas, and 0.4% for the prostate. These results showed that ID reduces with increasing tumor size for similar anatomic dimensions and the ID increases with increasing size of anatomical region for similar tumor sizes [1].

The human body is a structure that shows different density due to its chemical structural elements. Hounsfield Unit (HU) mean value is -1000 HU in air, +1000 HU in bone, -50 - 100 HU in fat tissue and -500 HU in lungs. Classically, the Hounsfield Unit values obtained from computerized tomography are calculated with the decrease of radiation in tissue using tables specific to predefined density ranges, and CT data, CT calibration curves. Algorithms and dose calculation mechanisms that may include tissue composition may have different accuracy in determining the dose in each organ.

In the Eclipse 13.0 treatment planning system (Varian Medical Systems, Palo Alto, CA), the Anisotropic Analytical Algorithm (AAA) method is commonly used for dose calculation [2] [3] [4] [5]. In the literature, there are studies reporting that the calculated doses of AAA were significantly incorrectly calculated. Near the two mediums, especially in the transition from tissue to air, it was seen that the dose was incorrectly calculated [6]. Recently, a new dose calculation algorithm, Acuros XB (Varian Medical Systems, Palo Alto, CA), is started to be used in clinic to correct this situation. AXB uses a complex technique to solve Linear Boltzmann Transport Equation (LBTE) and provides an accurate approach to the calculation of patient dose in heterogeneities originating entirely from lung, bone, air and different density implants [7] [8] [9] [10]. LBTE defines the macroscopic behavior of the radiation beam in the medium through which they pass.

Up to now, the effect of the difference between AAA and AXB on breast radiotherapy is not known due to different uses and further research is required to explain this effect. The difference in calculation between the two algorithms, which is affected by parameters such as the energy of the incoming beam, the field size and the electron density of the medium, reveals dose responses.

The aim of this study is to investigate the effect of the calculation differences between the AXB and AAA algorithms on the integral doses of critical organs in the radiotherapy of patients who underwent breast-conserving surgery due to breast cancer.

2. Materials and Methods

2.1. Eclipse Treatment Planning System

Eclipse TPS 13.0 (Varian, Palo Alto, California, USA) is designed for performing KRT, IMRT, VMAT, SRS/SBRT and electron plannings. The Eclipse treatment planning system in our clinic includes Dose Volume Optimization (DVO), Plan Geometry Optimization (PGO), Progressive Resolution Optimizer (PRO), Multi-Resolution Dose Optimization (MRDC) Algorithms, Pencil Beam Convolution (PBC), Analytical Anisotropic Algorithm (AAA) and Acuros XB (AXB) dose calculation algorithms.

2.2. Analytical Anisotropic Algorithm

The AAA dose calculation model is a 3D pencil beam and convolution superposition algorithm consisting of separate models for electrons emitted from primary photons, scattered photons, and beam modulators (primary collimator, beam straightening filter, and wedge filter). The functional forms for the basic physical quantities initiate a process by adding device properties to the account. This often leads to a noticeable reduction in the calculation time required for such algorithms. Tissue heterogeneities are added to calculation as anisotropic using photon scattering kernels of the multiple lateral direction in the 3D neighborhood. The final dose distribution is formed by superimposing the contribution of photons and electron beams. The dose behind the air gap is a little over-calculated in the AAA algorithm with an error caused by the modeling of the scattered dose.

2.3. Acuros XB Algorithm

The Acuros XB (AXB) algorithm was developed for two strategic needs such as accuracy and speed in external photon beam treatment planning. AXB uses a complex technique to solve Linear Boltzmann Transport Equation (LBTE) and clarifies the patient dose calculation for heterogeneities originating entirely from lung, bone, air, and non-biological implants. LBTE, which is the linear form of the Boltzman Transport Equaiton (BTE) and defines the macroscopic behavior of the radiation particles, assumes that the interaction of the radiation particles in the medium is formed without interaction of each other and an external

magnetic field. There are two solution approaches that try to explain LBTE. One of them is the Monte Carlo method, which does not clearly solve the commonly known LBTE and produces indirect solutions for LBTE. Second one is solving LBTE using numerical methods.

Monte Carlo and LBTE solution methods produce close results but fail to produce clear solutions, and mistakes are occurred. The mistakes of Monte Carlo System are random and result from the fact that a limited number of particles are simulated. Systematic faults can occur when using Monte Carlo methodologies to expedite the solution time.

The source model of the AXB algorithm used in Eclipse TPS uses the existing AAA resource model. Within this model; there are primary photons, out-of-focus photons, contaminated electrons and scattered photons.

The AXB algorithm uses the mass density information obtained from the CT images in each voxel for dose calculation.

2.4. Phantom Study

In order to measure the dosimetric difference between Analytical Anisotropic Algorithm and Acuros XB, measuring assembly was prepared as in **Figure 1** and the 2 mm spaced computed tomography images were taken. A 5 cm Styrofoam layer was used to obtain the air cavity (HU = -1000) in measuring assembly. CT images of the measuring device were transferred to the Eclipse TPS. The calculation was made at the calculation grid size (CGS) of 2.5 mm for the SSD: 100 cm, 10 × 10 area and at 6 MV for the AAA and AXB. Dose measurement information at specified measurement points were recorded. At the same conditions, the point dose measurements were made with 0.015 cm³ pin point ion chamber (PTW, Freiburg-Germany) at predetermined measuring points by being performed irradiation in Trubeam STx device.

2.5. Treatment Planning of Patients

Planning CT scans of 20 patients with early-stage left breast cancer, after breast-conserving surgery, were used for this study (**Table 1**). Data were generated with patients in the supine position with one arm above the head in the breast board. For the treatment planning, the 7-field IMRT was planned with 6 MV rays of the Varian TrueBeam STx device in the Eclipse treatment planning system. Two treatment planning were made for each patient plan using AAA and AXB algorithms. The calculation grid size (CGS) of 2.5 mm was chosen for all plans to minimize errors due to calculation grid size (CGS) in treatment volume.

The median dose of target volume was 50.4 Gy in 1.8 Gy fractions (46.8 - 50.4 Gy). An additional dose of 10 Gy (200 cGy × 5 fractions) was given to the lumpectomy cavity of some patients. If necessary, the conventional photon rays of 10 MV were used with 6 MV for planning. The tissue heterogeneity corrections were used in all calculations.

Table 1. Planning CT scans of 20 patients with early-stage left breast cancer, after breast-conserving surgery, were used for this study. Data were generated with patients in the supine position with one arm above the head in the breast board.

PATIENT CHARACTERISTICS	N = 20
MEAN AGE (RANGE)	52 (36 - 71)
STAGE 1	14
2	6
TUMOR LOCATION UPPER LATERAL	10
UPPER MEDIAL	2
LOWER LATERAL	7
LOWER MEDIAL	1
TUMOR SUBTYPE INVASIVE DUCTAL	15
INVASIVE LOBULAR	3
PAPILLARY	1
METAPLASTIC	1

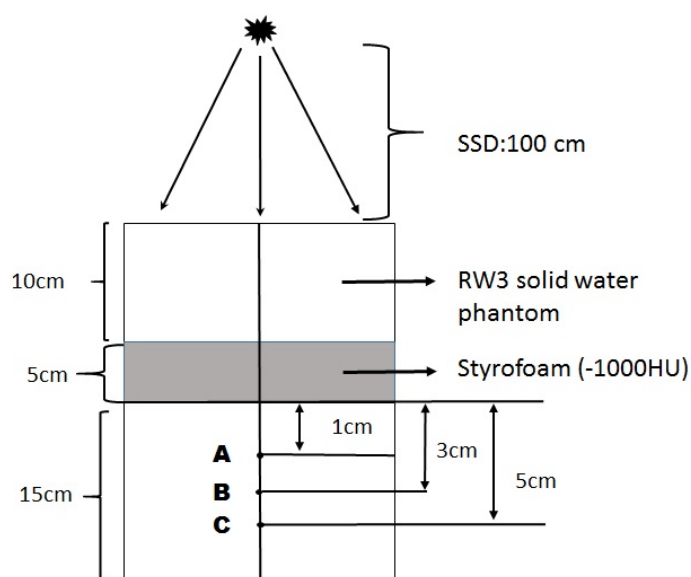


Figure 1. Experimental measurement assembly, SSD = 100 cm, 10 × 10 cm gap field, RW3 solid water phantom and 5 cm Styrofoam (-1000 HU). A measurement point: Point dose in a 1 cm area after tissue-air transition, B measurement point: Point dose in a 3 cm area after tissue-air transition, C measurement point: Point dose in a 5 cm area after tissue-air transition.

2.6. Evaluation of Dose Volume Histograms

Dose volum histograms (DVH) were evaluated for RTOG target volumes and OARs of each patient plan. While the treatment of the patients was being planned, the primary dose limitation was 95.0% of the target and 95.0% of the dose prescribed for chest or chest wall was provided to be received as PTV_{breast} .

From each patient's treatment planning; the V_5 Gy, V_{20} Gy, mean (D_{mean}) doses were calculated for the ipsilateral lung, V_{10} Gy, V_{20} , V_{30} Gy and D_{mean} for the heart, V_5 , V_{10} and D_{mean} for the contralateral breast, V_5 , V_{10} and D_{mean} doses for the contralateral lung. Besides all these; Body-PTV doses which are not in the RTOG criteria were calculated. V_5 and V_{20} doses were calculated separately for both algorithms, and small dose-volume responses of algorithms were investigated.

3. Results and Discussion

3.1. Evaluation of Phantom Measurements

In the measuring assembly shown in **Figure 1** which we prepared to demonstrate the differences in calculation between Analytical Anisotropic Algorithm and Acuros XB, the difference in dose between AAA and TPS was found to be 4% in A, which is the first dose measurement point after 5 cm air cavity, 7.8% in B, which is the second dose measurement point, and 9.5% in C.

Similarly; with AXB at the same measuring points, we achieved a difference of 1% at point A, 1.8% at point B and 3% at point C.

3.2. Evaluation of Dose-Volume Histograms

The dosimetric results for the treatment plan of 20 breast cancer patients formed using two different algorithms, are shown in **Table 2**. PTV_{breast} minimum, $PTV_{\text{breast}} D_{\text{mean}}$, $PTV_{\text{breast}} D_{95\%}$ doses; V_5 Gy, V_{20} Gy and D_{mean} doses for the contralateral lung; V_{10} Gy, V_{20} , V_{30} Gy and D_{mean} doses for the heart; V_5 , V_{10} and D_{mean} doses for the contralateral breast; V_5 , V_{10} and D_{mean} doses for the contralateral lung are shown in **Table 2**.

In **Table 2**; V_5 and V_{20} doses are shown separately for both algorithms by calculating the Body-PTV doses, which are not in the RTOG criteria.

Dose-Volume Histogram (DVH) for a patient calculated using the AAA and AXB dose algorithms is shown in **Figure 2**. There was a difference of 13% between the $PTV_{\text{breast}} D_{\text{min}}$ doses calculated by the AAA and AXB algorithms ($p < 0.05$). This may be related to the fact that the PTV_{breast} volume was calculated as high by the AAA algorithm although the PTV_{breast} volume was removed by 0.5 cm from the skin. There was no significant difference between the $PTV_{D95\%}$ doses calculated by the AAA and AXB algorithms ($p > 0.05$).

There was a significant difference between the V_5 , V_{20} and D_{mean} doses calculated by AXB and AAA algorithms for the left side lung ($p < 0.05$). V_5 , V_{20} and D_{mean} doses of the left side lung are higher in all AAA plans than the dosimetric results of the AXB plans.

There was a significant difference between the V_{10} , V_{20} , V_{30} and D_{mean} doses of the heart in all the plans of the AAA and AXB algorithms ($p < 0.05$).

Figure 3 shows comparison of dose distribution calculated using AAA and AXB dose calculation algorithms for a patient early-stage left breast cancer. The same 7 field IMRT plan recalculated using the AXB dose calculation algorithm (for the same patient, with the same dose scale).

Table 2. $PTV_{breast} D_{min}$: The minimum dose of PTV_{breast} volume, $PTV_{breast} D_{mean}$: The mean dose of PTV_{breast} volume, $PTV_{breast} D_{95\%}$: The dose prescribed to the 95% isodose line for the PTV_{breast} , V_5 : % Volume receiving dose of 5 Gy, V_{10} : % Volume receiving dose of 10 Gy, V_{20} : % Volume receiving dose of 20 Gy, V_{30} : % Volume receiving dose of 30 Gy, **Body-PTV**: The volume remaining after the removal of the PTV volume from the total body volume.

	AAA Dose(cGy) Ort ± SD	AXB Dose(cGy) Ort ± SD	p value	Integral Dose AAA (cGy*cm ³) Ort ± SD	Integral Dose AXB (cGy*cm ³) Ort ± SD	p value
$PTV_{breast} D_{min}$	3006 ± 125	2600 ± 105	0.001			
$PTV_{breast} D_{mean}$	5400 ± 125	5310 ± 108	0.021			
$PTV_{breast} D_{95\%}$	4870 ± 15	4810 ± 12	0.034			
Left Lung D_{mean}	1185 ± 12	1133 ± 8	0.003	1,265,561 ± 418	1,245,455 ± 287	0.001
Left Lung (V_5)	79 ± 3	72 ± 3	0.004			
Left Lung (V_{20})	14.9 ± 2	14.2 ± 2.3	0.002			
Heart D_{mean}	619 ± 4.2	604 ± 2.4	0.002	318.785 ± 344	312.605 ± 225	0.002
Heart (V_{10})	8.7 ± 2.1	8.5 ± 1.8	0.004			
Heart (V_{20})	4.8 ± 1.2	4.5 ± 1.1	0.003			
Heart (V_{30})	3.8 ± 1	3.4 ± 1	0.004			
Contralateral breast D_{mean}	202 ± 2.3	185 ± 2.2	0.003	205.838 ± 25	188.515 ± 24	0.003
Contralateral breast (V_5)	4.7 ± 2.2	3.3 ± 2.1	0.001			
Contralateral breast (V_{10})	0.6 ± 0.2	0.7 ± 0.1	0.034			
Contralateral Lung D_{mean}	289 ± 4	277 ± 2.1	0.001	362.406 ± 25	347.358 ± 18	0.002
Contralateral Lung (V_5)	12 ± 1.1	11.4 ± 1.1	0.004			
Contralateral Lung (V_{10})	0.70 ± 0.1	0.62 ± 0.1	0.003			
Body-PTV (V_5)	24.2 ± 1.6	24 ± 1.7	0.250			
Body-PTV (V_{20})	10.8 ± 1.1	10.9 ± 1.2	0.320			

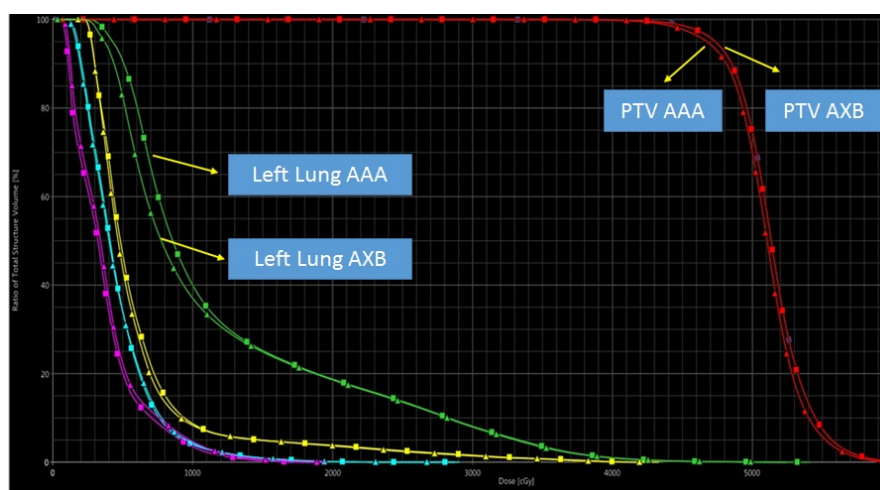


Figure 2. Dose Volume Histogram (DVH) of PTV, contralateral breast, heart, left lung and right lung for a patient with 1850 cm³ PTV calculated using AAA and AXB algorithms.

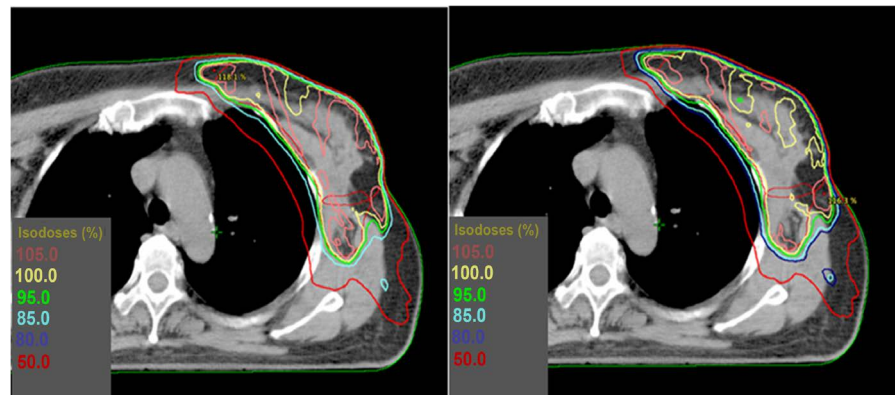


Figure 3. Comparison of dose distribution calculated using AAA and AXB dose calculation algorithms for early-stage left breast cancer. Left: Axial slice of 7 field IMRT plan calculated using AAA showing the dose distribution for a left side breast cancer. The dose colour scale ranges from 50% (red) to 105% (brown) of the normalized dose 95% prescribed dose of 50 Gy. Right: The same 7 field IMRT plan recalculated using the AXB dose calculation algorithm (for the same patient, with the same dose scale).

When D_{mean} doses of the contralateral lung doses were evaluated, there was a significant difference between AAA plans and AXB plans ($p < 0.05$). There was also a significant difference between the doses of V_5 and V_{10} in the contralateral lung ($p < 0.05$).

There was a significant difference between the D_{mean} , V_5 and V_{10} doses of the contralateral breast ($p < 0.05$).

Finally; in our study comparing the V_5 and V_{20} doses for Body-PTV, it was found that there was no significant relationship between AAA plans and AXB plans ($p > 0.05$).

Huang *et al.* showed that the calculation grid size (CGS) was related to the dose estimation in their studies of the lung stereotactic radiotherapy (SBRT) planning [11]. To reduce this effect in our study, all plans for both algorithms were calculated at 2.5 mm CGS.

In a planning study performed for nasopharyngeal cancers by Kan *et al.*, they reported that a lower dose between 3% and 6% was obtained with AXB on critical organs compared to AAA [12].

Chung and Mittauer showed that CGS was effective on dose estimation for head and neck treatments [13] [14]. Ong *et al.* reported that the 1.0 mm CGS performed a more accurate dose calculation than the 2.5 mm CGS in AAA calculations [15].

In our dosimetric phantom study, we detected that there was a 3% compliance was between the depth dose measurement and Acuros AXB algorithm. However, we found there was a dose difference of 9.5% between the depth dose measurement and AAA algorithm.

In the phantom study with 6 MV photon rays by Bush *et al.*, they showed that there was difference of 4.5% between AXB and Monte Carlo algorithms in the transition from air to tissue and this difference increased to 13% between AAA and Monte Carlo algorithms [16]. In parallel with this study, Kan *et al.* found

that there was a difference of 3% between the measurement and AXB algorithm in the transition from air to tissue and this difference reached 10% with AAA algorithm (12). In the random phantom study developed for head and neck treatments by Han *et al.*, they found the maximum difference between measurement and calculation as 4.6% for AAA and 3.6% for AXB [17].

In a study comparing the treatment plans of deep inspiration condition and free-breathing breast patients by Fogliata *et al.*, they showed that Anisotropic Analytical Algorithm calculated a 1.6% more dose in PTV than Acuros XB [18].

Padmanaban *et al.* compared the AAA and AXB algorithms using 3D Conformal and Rapid Arc techniques in the treatment of oesophagus cancers and they found that the AXB algorithm determined a low dose in PTV (0.5 - 1.3 Gy) according to AAA. They showed that the low dose in PTV obtained for AXB was not related to the technique used [19].

4. Conclusions

The most remarkable side of our study is that the dose of breast tissue that starts immediately after the skin was calculated as higher with the AAA algorithm. There was a difference of 13% between AAA plans and AXB plans in determining PTV min dose. The AAA algorithm calculated a higher dose than should be in the build-up area between air and tissue. The higher dose should be in PTV, and will increase the maximum dose effect in the hot dose regions as a result of the normalization of the plan to the treatment dose.

The integral dose (ID) is the volume integral of the dose stored in a medium and it is equal to multiplication of the mean dose (D_{mean}) and volume in the medium. Often, the large number of beams and high irradiation times used in the IMRT cause an increase in the ID and this increase in the ID is prevented by using high energy photon rays. In the literature, there is no study comparing integral doses of healthy organs between AAA and AXB algorithms.

Our study revealed that the calculation differences between Acuros XB (AXB) and Anisotropic Analytical Algorithm (AAA) in breast radiotherapy caused serious differences on the stored integral doses on critical organs.

As a result; in the region where we are pushing critical dose limits such as skin, lung, heart, and contralateral breast, the administering of breast radiotherapy and the accuracy of dose delivery are very difficult due to both anatomical and different density tissues. In addition to very different tissue densities within the treatment area, many devices that increase the dosimetric uncertainty associated with the patient stabilizing devices found that the outside treatment area affects the dose in the patient. It should be kept in mind that treatment planning algorithms do not yet have the ability to accurately calculate the dose in air-tissue transition zones.

Conflicts of Interest

None.

References

- [1] D'Souza, W.D. and Rosen, I.I. (2003) Nontumor Integral Dose Variation in Conventional Radiotherapy Treatment Planning. *Medical Physics*, **30**, 2065-2071. <https://doi.org/10.1118/1.1591991>
- [2] Tillikainen, L., Siljamäki, S., Helminen, H., Alakuijala, J. and Pyyry, J. (2007) Determination of Parameters for a Multiple-Source Model of Megavoltage Photon Beams Using Optimization Methods. *Physics Medicine in Biology*, **52**, 1441-1467. <https://doi.org/10.1088/0031-9155/52/5/015>
- [3] Breitman, K., Rathee, S., Newcomb, C., Murray, B., Robinson, D., Field, C., *et al.* (2007) Experimental Validation of the Eclipse AAA Algorithm. *Journal of Applied Clinical Medical Physics*, **10**, 76-92.
- [4] Tillikainen, L., Helminen, H., Torsti, T., Siljamäki, S., Alakuijala, J., Pyyry, J. and Ulmer, W. (2008) A 3D Pencil-Beam-Based Superposition Algorithm for Photon Dose Calculation in Heterogeneous Media. *Physics in Medicine and Biology*, **53**, 3821-3839. <https://doi.org/10.1088/0031-9155/53/14/008>
- [5] Van Esch, A., Tillikainen, L., Pyykkonen, J., Tenhunen, M., *et al.* (2006) Testing of the Analytical Anisotropic Algorithm for Photon Dose Calculation. *Medical Physics*, **33**, 4130-4148. <https://doi.org/10.1118/1.2358333>
- [6] Robinson, D.M. (2008) Inhomogeneity Correction and the Analytical Anisotropic Algorithm. *Journal of Applied Clinical Medical Physics*, **9**, 112-122. <https://doi.org/10.1120/jacmp.v9i2.2786>
- [7] Vassiliev, O., Wareing, T., McGhee, J., Failla, G., Salehpour, M. and Mourtada, F. (2010) Validation of a New Grid-Based Boltzmann Equation Solver for Dose Calculation in Radiotherapy with Photon Beams. *Physics Medicine in Biology*, **55**, 581-598.
- [8] Hoffmann, L., Jørgensen, M., Muren, L. and Petersen, J. (2012) Clinical Validation of the Acuros XB Photon Dose Calculation Algorithm, a Grid-Based Boltzmann Equation Solver. *Acta Oncologica*, **51**, 376-385. <https://doi.org/10.3109/0284186X.2011.629209>
- [9] Fogliata, A., Nicolini G., Clivio, A., Vanetti, E. and Cozzi, L. (2011) Dosimetric Evaluation of Acuros XB Advanced Dose Calculation Algorithm in Heterogeneous Media. *Radiation Oncology*, **6**, 82. <https://doi.org/10.1186/1748-717X-6-82>
- [10] Han, T., Mikell, J., Salehpour, M. and Mourtada, F. (2011) Dosimetric Comparison of Acuros XB Deterministic Radiation Transport Method with Monte Carlo and Model-Based Convolution Methods in Heterogeneous Media. *Medical Physics*, **38**, 2651-2664. <https://doi.org/10.1118/1.3582690>
- [11] Huang, B., Wu, L.L., Pei, X.L. and Chen, C.Z. (2015) Dose Calculation of Acuros XB and Anisotropic Analytical Algorithm in Lung Stereotactic Body Radiotherapy Treatment with Flattening Filter Free Beams and Potential Role of Calculation Grid Size. *Radiation Oncology*, **10**, 53. <https://doi.org/10.1186/s13014-015-0357-0>
- [12] Kan, M., Leung, L. and Yu, P. (2012) Verification and Dosimetric Impact of Acuros XB Algorithm on Intensity Modulated Stereotactic Radiotherapy for Locally Persistent Nasopharyngeal Carcinoma. *Medical Physics*, **39**, 4705-4714. <https://doi.org/10.1118/1.4736819>
- [13] Chung, H., Jin, H., Palta, J., Suh, T.S. and Kim, S. (2006) Dose Variations with Varying Calculation Grid Size in Head and Neck IMRT. *Physics Medicine in Biology*, **51**, 4841-4856.
- [14] Mittauer, K., Lu, B., Yan, G., Kahler, D., Gopal, A., Amdur, R., *et al.* (2013) A Study

- of IMRT Planning Parameters on Planning Efficiency, Delivery Efficiency, and Plan Quality. *Medical Physics*, **40**, Article ID: 061704. <https://doi.org/10.1118/1.4803460>
- [15] Ong, C.L., Cuijpers, J.P., Senan, S., Slotman, B.J. and Verbakel, W.F. (2011) Impact of the Calculation Resolution of AAA for Small Fields and RapidArc Treatment Plans. *Medical Physics*, **38**, 4471-4479. <https://doi.org/10.1118/1.3605468>
- [16] Bush, K., Gagne, I.M., Zavgorodni, S., Ansbacher, S. and Beckham, W. (2011) Dosimetric Validation of Acuros XB with Monte Carlo Methods for Photon Dose Calculations. *Medical Physics*, **38**, 2208-2221. <https://doi.org/10.1118/1.3567146>
- [17] Han, T., Mourtada, F., Kisling, K., Mikell, J., Followill, D. and Howell, R. (2012) Experimental Validation of Deterministic Acuros XB Algorithm for IMRT and VMAT Dose Calculation with Radiological Physics Center's Head and Neck Phantom. *Medical Physics*, **39**, 2193-2202. <https://doi.org/10.1118/1.3692180>
- [18] Fogliata, A., Nicolini, G., Clivio, A., Vanetti, E. and Cozzi, L. (2011) On the Dosimetric Impact of Inhomogeneity Management in the Acuros XB Algorithm for Breast Treatment. *Radiation Oncology*, **6**, 103. <https://doi.org/10.1186/1748-717X-6-103>
- [19] Padmanaban, S., Warren, S., Walsh, A., Partridge, M. and Hawkins, A. (2014) Comparison of Acuros (AXB) and Anisotropic Analytical Algorithm (AAA) for Dose Calculation in Treatment of Oesophageal Cancer: Effects on Modelling Tumour Control Probability. *Radiation Oncology*, **9**, 286.